

# Report on performance, energy balances and design criteria for salt gradient power reverse electro dialysis

## CHPM2030 Deliverable D3.3

Version: August 2018



CHPM2030



This project has received funding from the European Union's Horizon 2020 research and innovation programme under grant agreement n° 654100.



**Author contact**

*Joost Helsen*

*VITO*

*Boeretang 200*

*2400 Mol*

*Belgium*

*Email: [joost.helsen@vito.be](mailto:joost.helsen@vito.be)*

**Published by the CHPM2030 project, 2018**

*University of Miskolc*

*H-3515 Miskolc-Egyetemváros*

*Hungary*

*Email: [foldshe@uni-miskolc.hu](mailto:foldshe@uni-miskolc.hu)*





## CHPM2030 DELIVERABLE D3.3

### REPORT ON PERFORMANCE, ENERGY BALANCES AND DESIGN CRITERIA FOR SALT GRADIENT POWER REVERSE ELECTRODIALYSIS

#### *Summary:*

This deliverable was produced in the framework of the activities in WP3 related to surface technologies for the CHPM2030 concept. It covers the experimental work carried out in view of demonstrating the technical feasibility of applying reverse electrodialysis to extract electrical energy from the geothermal brine. It contains the results of an extensive lab study and subsequent pilot test with both artificial and real brines.

#### *Authors:*

Joost Helsen (VITO)  
Elisabeth Andres Garcia (VITO)  
Jan Stroobants (VITO)  
Christof Porto-Carrero (VITO)  
Diane Van Houtven (VITO)



## TABLE OF CONTENTS

1	Executive summary .....	4
2	Introduction .....	5
2.1	Scope and objectives of the activities related to D3.3. ....	5
2.2	Salinity gradient power via reverse electrodialysis .....	5
2.3	Geothermal brine composition .....	7
3	Lab experiments .....	9
3.1	Materials and methods .....	9
3.1.1	Ion conductive membranes .....	9
3.1.2	Three compartment set-up and data acquisition.....	10
3.1.3	Data processing .....	12
3.2	Results and discussion .....	14
3.2.1	Experiments with pure NaCl .....	14
3.2.2	Experiments at increased temperature.....	16
3.2.3	Experiments with multivalent ions.....	21
3.2.4	Experiments with multivalent ion combinations at increased temperature .....	23
4	Pilot scale experiments .....	25
4.1	Materials and methods .....	25
4.2	Results and discussion .....	31
5	Conclusions .....	32
6	References .....	33
7	Glossary.....	35

## LIST OF FIGURES

Figure 1 Schematic drawing of reverse electrodialysis .....	6
Figure 2 Schematic view of the 3-compartment set-up .....	11
Figure 3 Three-compartment cell and setup including peristaltic pumps and heat exchangers .....	12
Figure 4 Conductivity vs concentration curve of NaCl solutions (25°C).....	13
Figure 5 Power density (left) and current density (right) as a function of the concentration of HIGH and LOW for FUJI membranes.....	15
Figure 6 Power density (left) and current density (right) as a function of the concentration of HIGH and LOW for FKE/FAS membranes.....	15
Figure 7 Power density (left) and current density (right) as a function of the concentration of HIGH and LOW for FKS/FAS membranes.....	16
Figure 8 FKE/FAS @ increased temperature half-cell potential and permselectivity.....	17
Figure 9 FKE/FAS @ increased temperature: power and current density results .....	18
Figure 10 FUJI @ increased temperature: half-cell potential and permselectivity results .....	19
Figure 11 FUJI @ increased temperature power and current density results .....	20
Figure 12 Experimental results FUJI membranes: influence of Ca and Mg.....	22
Figure 13 Experimental results FKS/FAS membranes: influence of Ca and Mg .....	22
Figure 14 Experimental results of combined test (Ca+Mg) with FKE/FAS: current- and power density as a function of temperature.....	23
Figure 15 Comparison of reference test results and combined test (Ca+Mg) with FKE/FAS: current- and power density as a function of temperature .....	24
Figure 16 SGP-RE pilot plant: instrumentation side .....	25
Figure 17 SGP-RE pilot plant: tank side (ELEC, HIGH, LOW, from left to right) .....	25
Figure 18 Screen shot of MeFiAS software.....	27
Figure 19 Typical Voltage-current and power density-current density graphs during galvanostatic experiments .....	29

## LIST OF TABLES

Table 1 Potential brine sources for SGP-RE.....	6
Table 2 Brine composition for geothermal sites in France-Germany and Belgium .....	7
Table 3 Composition of an artificial brine, based on data from Belgium and France.....	8
Table 4 Properties of selected ion exchange membranes .....	10
Table 5 Overview of experiments with pure NaCl .....	14
Table 6 Pure NaCl experiments: overview of half-cell potential and apparent permselectivity .....	14
Table 7 Overview of experiments at increased temperature.....	16
Table 8 Overview of experiments with multivalent ions.....	21
Table 9 Overview of experiments with multivalent ions at increased temperature.....	23
Table 10 Reference conditions (25°C and 50°C).....	30
Table 11 Experimental conditions for the SGP-RE pilot testing .....	30

## 1 Executive summary

In the provisioned CHPM technology an enhanced geothermal system would be established on a deep metal-bearing geological formation, which would be conducted in a way that the co-production of energy and metals could be possible. The aim of this study is to demonstrate the technical feasibility of the extracting surplus electrical energy from the geothermal brine. Chemical energy is stored in the brine as in the form of dissolved salts. Using a process called 'reverse electrodialysis' this energy can be tapped. Reverse electrodialysis (RE) has been tested at pilot scale for river water, sea water and concentrated brine applications. Extracting salt gradient power (SGP) from geothermal brines is a new concept, launched in this project.

To establish a first technical feasibility a few important keys were identified to unlocking the hidden potential of salinity gradient energy extraction. The specific characteristics of a geothermal brine that first come to mind when envisaging application of 'reverse electrodialysis' are the temperature and the composition of the brine. The temperature can create extra leverage in to extracting the energy and is generally considered a 'free win'. Geothermal brines -especially ultradeep ones- are rich in dissolved species, such as gases, metals and salts. General rule is that the depth of the brine is determining the salt content and on specific locations also the metal content. High salt content favours high energy output from the SGP-RE. There is a catch however; presence of multivalent ions can jeopardize the energy extraction potential. The way the CHPM2030-concept is conceived partially takes this consideration into account. Two metal extraction technologies are foreseen to recover the metals from the brine, therefore making it more suitable for SGP-RE. On the other hand other multivalent ions such as alkaline earth metals will still be present and the effect should be studied to anticipate potential problems.

A specific lab-scale setup to test a single cell pair SGP-RE system was designed and built for investigating the applicability of the process. Four steps were taken to elucidate the most important factors influencing the performance: examination of the performance of three commercially available membrane pairs (1), effect of increased temperature (2); effect of multivalent ions (3), combined effect of multivalent ions and increased temperature (4).

Testing three combinations of commercially available ion exchange membranes in the lab setup it revealed that FUJI membranes were the most performant at high salt concentration, but their performance dropped significantly when the brine concentration lowered. The other two pairs were more suitable at moderate to low concentrations and also less prone to a decrease in concentration of the brine.

The experiments at increased temperature showed a very clear benefit of using geothermal brines at 60°C or even higher. The power density of the FKE/FAS membranes at high temperatures increased 10 times compared to the tests at room temperature, even though the cell potential was less than expected due to a deteriorating permselectivity at high temperatures.

The final lab experiments consisted of determining the effect of multivalent ions on the performance. Calcium and Magnesium were chosen as the most common multivalent cations observed in real brines. The effect was studied on the FUJI and FKE/FAS membrane pairs. It was found that the presence of Ca and Mg had little or no effect on the cell potential (given equal molarities). As a single salt, neither Ca nor Mg had a big influence on the performance of the single cell. In a combined set of experiments however it was found that the performance reduced significantly when both cations ( $\text{Ca}^{2+}$ ,  $\text{Mg}^{2+}$ ) were present. In those cases the performance was reduced approximately 50%, compared to the case without multivalent ions. This performance loss was consistent throughout the entire temperature range that was studied (25-60°C).

## 2 Introduction

### 2.1 Scope and objectives of the activities related to D3.3.

The main objective of task 3.3. was to check the technical feasibility of reverse electrodialysis to enhance the electrical power output of the EGS. Geothermal brines -especially originating from an ultra-deep EGS- typically have high salt content which could be used as 'fuel' for extracting a surplus of energy on top of the energy produced through the binary cycle of the EGS. In order to do so, the geothermal brine should be contacted with a low salinity water source, e.g. surface water, treated waste water, shallow ground water etc.

The rationale behind exploiting the chemical potential of the geothermal brine consists of the following elements:

- Deep geothermal brines exhibit often very high concentrations of salts. Higher concentration indicates more chemical energy is stored in the brine
- The inherently high temperatures of the geothermal brines make them more suitable for electricity production via reverse electrodialysis
- The technology can be easily integrated in the closed loop of the EGS. Although there is no direct contact between the brine and the low salinity source, salts are transferred to the low salinity source. Moreover water transport also occurs as a result of osmotic and electroosmotic transport.

Application of reverse electrodialysis in EGS can be restricted by the following aspects:

- Low performance when the salinity of the geothermal brine is too low compared to the low-salinity water source
- Presence of multivalent ions in the geothermal brine that could decrease the power output
- Presence of other elements in the brine that could be hazardous to the environment
- The availability of a low salinity water source
- The possibility to discharge the salt-enriched water in a sustainable manner

The scope of this experimental study was to elucidate the potential of salt gradient power applied to geothermal brines and study the following effects on the performance of the process:

- the concentration of the brine and the low salinity water source
- the most predominantly present multivalent ions
- the temperature

The experiments were carried out on lab- and pilot scale. The lab scale setup offered the advantage of swift and easy membrane replacement in order to test different membranes in different conditions. The pilot scale installations give a more realistic projection of the performance of the technology in real-life conditions. Its operation is similar to a full-scale SGP-RE plant. The details of both setups are described in the respective sections.

### 2.2 Salinity gradient power via reverse electrodialysis

Renewable energy sources are required for reducing pollution, carbon dioxide emissions, and the fossil energy part in global energy consumption. Harvesting energy from the environment in a sustainable way to satisfy the growing energy demand of the human society is primordial for the surviving and sustainable development of mankind. Technologies for harvesting renewable energy such as solar, wind and geothermal sources have attracted great attention and have been developed extensively in recent years. The energy stored as the salinity difference between two sources exhibiting different salinities is another large-scale renewable energy source that can be exploited. Examples of saline sources can be seawater, RO brines, saline groundwater, saline industrial effluents, salt ponds, etc. Extraction of salinity gradient energy efficiently still

remains a challenge. With the development of membrane science and technology, membrane-based techniques for energy extraction from saline sources, such as pressure-retarded osmosis and reverse electro-dialysis, have made big leaps in recent years.

Table 1 Potential brine sources for SGP-RE

Brine source	Brine concentration	Flow rate	Theoretical potential
Great Salt Lake (Ohio, US)	100-300g/l	125m <sup>3</sup> /s	15,8 TWh/yr
Dead Sea and Red Sea	340g/l	25m <sup>3</sup> /s	2,6 TWh/yr
Garabogazköl Aylagy	350g/l	25m <sup>3</sup> /s	2,7 TWh/yr
RO SWDU	40-100g/l		
Chlor-alkali	210-250g/l		
Salt ponds	250-300g/l		
<b>Geothermal brine</b>	<b>1-300g/l</b>	<b>?</b>	<b>?</b>

Reverse ElectroDialysis (RED) uses a similar process design as in electrodialysis (ED). The only difference is in the operation of the process, instead of feeding the same solution in all the compartments, in a RED unit two solutions with different concentrations are fed alternatively in the compartments. An high concentration and a low concentration solutions are needed in order to make this electrochemical reactor to work. The membrane stack is made of cell pairs consisting of one CEM, one high-concentration channel, one AEM and one low-concentration channel each (Figure 1).

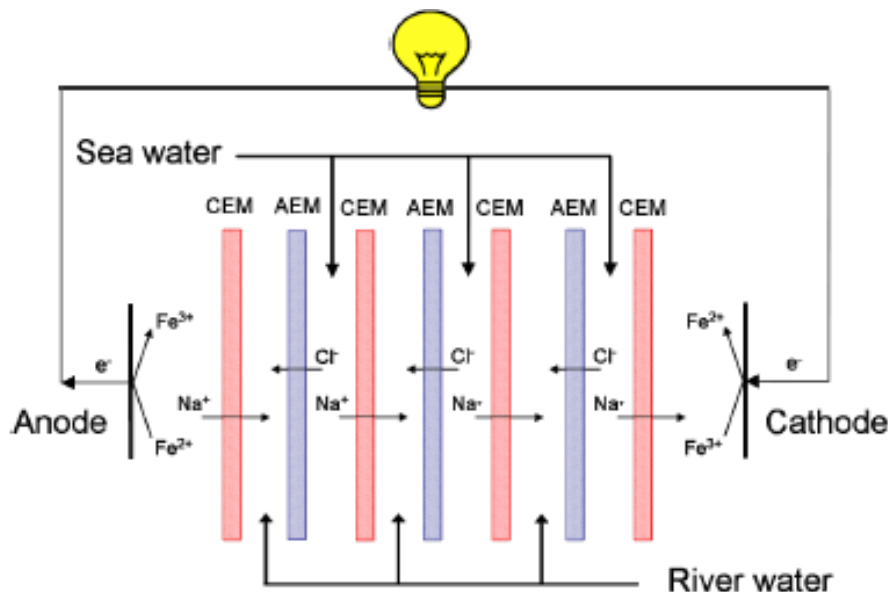


Figure 1 Schematic drawing of reverse electrodialysis

The concentration gradients across the membranes cause the ions to move in opposite directions, since  $\text{Na}^+$  can pass only through CEM and  $\text{Cl}^-$  only through AEM. Due to the transport of ions a potential difference is



generated across the membranes and within a cell pair. Adding the contribution of many cell pairs, it is possible to have a significant potential between the 'end-electrodes'. This potential difference can then trigger a redox reaction. The electrolyte rinsing solution (ERS) plays a fundamental role in the operation of the process since it converts the ionic current into an electronic one. This is enabled by the redox couple present in the ERS solution and which is recirculated continuously between anode and cathode. Connecting the anode and cathode with an external load will enable an electrical current to flow. Two DSA (Dimensionally Stable Anodes) are used as end-electrodes. They are inert electrodes and their role is to catalyse the reaction of the redox species.

### 2.3 Geothermal brine composition

Obtaining reliable information on brine composition is extremely cumbersome. At the start of task 3.3, little or no information was available on brine compositions and initial tests were therefore performed with pure NaCl solutions at concentrations varying between 1 and 5M. During the project and especially in the second period more detailed information became available that allowed a more detailed determination of the synthetic brine composition. Below in Table 2 compositions of two different geothermal brines are given from sites in France and Belgium. These are the most relevant for the CHPM2030 concept regarding well depth, respectively at 5000 and 3280 m depth. As can be seen from the figures, both brines show similar compositions in the dominating ions, such as: sodium, chloride, calcium, magnesium, sulphate, bicarbonate, iron, potassium and strontium.

*Table 2 Brine composition for geothermal sites in France-Germany and Belgium*

Place	France-Germany	Belgium
Place description	Upper Rhine Graben	Mol
Depth (m)	1547-5000	3280
pH	5.06-6.92	
Temperature (°C)	35-91.7	125
Conductivity (mS cm <sup>-1</sup> )	23-158	
TDS	15.6-201	
TIC	11.4-127	
TOC	0.7-35.2	
SiO <sub>2</sub>	35.8-201	102,5
H <sub>2</sub> SiO <sub>3</sub>		133,2
HCO <sub>3</sub>		1129
NH <sub>3</sub>	1.65-47.4 (NH <sub>4</sub> )	264 (NH <sub>4</sub> )
As	0.021-11.6	
Br	2.5-726	134
Cl	6375-120500	100200
F	0.85-31.8	<0.88
NO <sub>3</sub>	<0.5	
SO <sub>4</sub>	126-2730	380
PO <sub>4</sub>	<0.1-3.1	
Ag	<0.0001-0.0015	
Al	0.005-0.094	

Place	France-Germany	Belgium
B	3.9-45.9	
Ba	0.05-17.6	16,5
Be (ppb)	1.52-22.7	
Ca	719-11700	9130
Cd (ppb)	<0.1-55.9	
Co	<0.0005-0.005	
Cr (ppb)	<1-1.04	
Cs	0.204-19.3	
Cu	<0.001-0.372	
Fe	0.14-78.0	806
Ge (ppb)	10.3-70.4	
K	155-4030	2870
Li	4.5-210	
Mg	76.0-1930	560
Mn	0.015-26.1	13,6
Na	4400-64000	49600
Ni (ppb)	1.06-67.3	
Pb	<0.0005-3.39	
Rb	0.65-30.2	
Sb	0.0574-0.267	
Si		47,9
Sr	12.1-498	400
Th (ppb)	0.00019-0.00092	
Zn	0.018-15.2	
Nd (ppb)	0.13-0.538	
U (ppb)	0.007-0.033	
Reference	Sanjuan et al 206	Current study

Based on these data an 'artificial brine' was defined, containing the ions most relevant to the SGP-RE process and predominantly present in both brines. The composition of this brine is given in Table 2. Due to analytical error and simplification of the composition of the actual brines, the balance between anions and cations is slightly off. This can be adjusted by balancing between salts of the different cations (as shown in paragraph 3.1).

*Table 3 Composition of an artificial brine, based on data from Belgium and France*

		mM	mEq			mM	mEq
HCO <sub>3</sub>	1000	16	16	Ca	10000	250	500
Cl	100000	2817	2817	Fe	500	9	18
SO <sub>4</sub>	2000	21	42	K	3000	77	77
				Mg	1000	42	83
				Na	55000	2391	2391
				Sr	400	5	9
		<b>TOTAL -</b>	<b>2874,962</b>		<b>TOTAL +</b>		<b>3078,417</b>

### 3 Lab experiments

The lab experiments consisted of single cell pair experiments with two membranes, mimicking the complex phenomena happening in a full-scale reverse electrodialysis stack. Ultimately it gives information on the electrical potential across the membranes and the current that is generated. Combination of those two figures can be used as a good prediction tool for the electrical power that can be extracted from the cell pair in the given circumstances – such as salinity, temperature, etc.

The experiments first carried out were focussed on determining a promising couple of membranes for the further investigation. The initial tests were carried out at very high brine concentrations. During the course of the project it became clear that extremely high brine salinities (i.e. close to saturation) were probably unlikely to occur, so the focus was shifted towards medium salt concentration, as found in brines occurring from existing ultradeep wells. Based on more extensive analytical results from the real brines, the experiments were shifted towards the influence of multivalent ions, in particular Mg and Ca, and in the last stage towards higher temperatures as well. In total 38 experiments were carried out, in triplo or in duplo,

#### 3.1 Materials and methods

##### 3.1.1 Ion conductive membranes

Ion conductive membranes are made of a polymer from which it inherits its specific characteristics. The material consists of a polymer backbone (e.g. polystyrene) with fixed ions homogeneously distributed in the material as functional side groups along the polymer chain backbone [17]. In the case of a CM these functional groups are e.g.  $\text{SO}_3^-$  or  $\text{COO}^-$  groups while in the case of an AM these are e.g.  $^+\text{NH}_2\text{R}$  or  $^+\text{NHR}_2$  groups. Inherently, a homogeneous IEX membrane presents a uniform distribution of fixed ions in its structure. As a result, the concentration of migrating counterions needs to satisfy the electro-neutrality within the IEX membrane. In An IEX membrane can be considered as a passing-through medium: an incoming ion<sub>in</sub> at one side of the membrane causes another ion<sub>out</sub> to be expelled from the other side of the membrane. In the bulk of the membrane, the transport of ions can be considered as a simultaneous migration of a large number of counterions to neighbouring fixed ion positions in order to switch position -hopping- and to force the ejected ion<sub>out</sub> out of the membrane.

Membrane characteristics such as permselectivity, (electro-)migration coefficient and membrane thickness are important parameters that determine the SGP-RE battery power output. Direct measurements on a complete SGP-RE stack (as described in section 4.1) are evidently very important. But this takes a considerable effort in mounting a complete SGP-RE stack including a sufficient number of cell-pairs and adequate SGP-RE electrodes. It demands an important research investment (financial, technicians) and often leads to results that are very difficult to reproduce. Therefore VITO developed a pragmatic and alternative measurement within a three compartment set-up. This set-up allows to extract first crucial and practical information with respect to the global SGP-RE performance of a set of CM and AM membranes under certain conditions (composition and temperature of the fluids) within a cell pair, before testing those in more detail in a full (lab-scale) SGP-RE stack.

The membranes used in the 3-compartment setup were purchased at FUMATECH and FUJIFILM. The FUJIFILM membranes are homogenous membranes casted on a non-charged polymer non-woven structure for mechanical reinforcement. The FUJIFILM membranes are 160µm thick and specifically designed for energy generation purposes which amongst others implies a high permselectivity in high brine concentrations. The FUMATECH membranes are 20µm thick, homogenous membranes with no mechanical support. In [15,16] the importance of thin membranes is highlighted in order to create a high SGP-RE power density ( $\text{W/m}^2$ ) output. Thin membranes, though commercially available are not yet produced on an industrial scale. Two types of thin homogeneous CM and one type of a thin homogeneous AM materials were

tested: FKS20 (CM), FKE20 (CM) and FAS20 (AM). The two possible combinations of CM and AM were tested (FKS20/FAS20 and FKE20/FAS20). The main properties of the selected membranes are given in Table 4.

*Table 4 Properties of selected ion exchange membranes*

FUJI	AEM	CEM
<b>Type</b>	Anion exchange	Cation exchange
<b>thickness dry</b>	120 $\mu\text{m}$	120 $\mu\text{m}$
<b>Permselectivity (0.017 M – 0.5 M)</b>	96%	96%
<b>Permselectivity (0.5 M – 4 M)</b>	65%	90%
<b>Area Resistancea), <math>\Omega\cdot\text{cm}^2</math></b>	1,83	2,55

Fumasep	FAS – 20	FKS – 20	FKE – 20
<b>Type</b>	Anion exchange	Cation exchange	Cation exchange
<b>thickness dry</b>	18-22 $\mu\text{m}$	18-22 $\mu\text{m}$	18-22 $\mu\text{m}$
<b>selectivity 0.1/0.5 mol/kg of KCl at T=25°C<sup>a</sup>)</b>	95.5%	99.02%	95.8%
<b>area resistance in Cl- form<sup>b</sup>)</b>	0.5 $\Omega\cdot\text{cm}^2$	1.7 $\Omega\cdot\text{cm}^2$	0.66 $\Omega\cdot\text{cm}^2$
<b>dimensional swelling in H<sub>2</sub>O at T= 25°C<sup>c</sup>)</b>	0 – 2%	0 – 2%	0%

a) Determined from membrane potential measurement in a concentration cell

b) In Cl- form in 0,5 M NaCl @ T= 25°C, measured in standard measuring cell (through-plane)

c) In Br- form, membrane as received stored in water for 24 hrs, reference membrane as received.

### 3.1.2 Three compartment set-up and data acquisition

A set-up, as schematically depicted in Figure 2, was built. It consists of three compartments :

- compartment 1 is separated from compartment 2 through a CM
- compartment 2 is separated from compartment 3 through an AM

The HIGH solution is pumped to compartment 1, the outlet (HIGH\_OUT) of compartment 1 is connected to the inlet (HIGH\_IN) of compartment 3. The HIGH\_OUT of compartment 3 is connected to the pump\_IN, and therefore to the HIGH\_IN of compartment 1. Consequently the HIGH is continuously recycled as a batch volume through compartments 1 and 3. The LOW solution is pumped to compartment 2. The LOW\_OUT is recycled to the LOW\_IN, in order to also have a LOW batch experiment. As a result, a salinity gradient is created across both membranes from the difference in the HIGH and LOW concentration. This gradient causes the migration through the ion conductive membranes. The concentration of cations and anions thus will gradually increase in the LOW while the concentration in the HIGH will decrease accordingly. Hence the set-up allows to measure the overall and practical ion-migration kinetics for a specific pair of CM and AM. Therefore a three compartment set-up measurement, as described here, is a relevant characterisation method to extract SGP-RE related information for a specific pair of CM and AM. The CM and AM samples have an effective exposure diameter of 5 cm in the set-up. The width of each compartment is about 6 cm. In the centre of each of the three compartments the tip of a reference electrode is positioned.



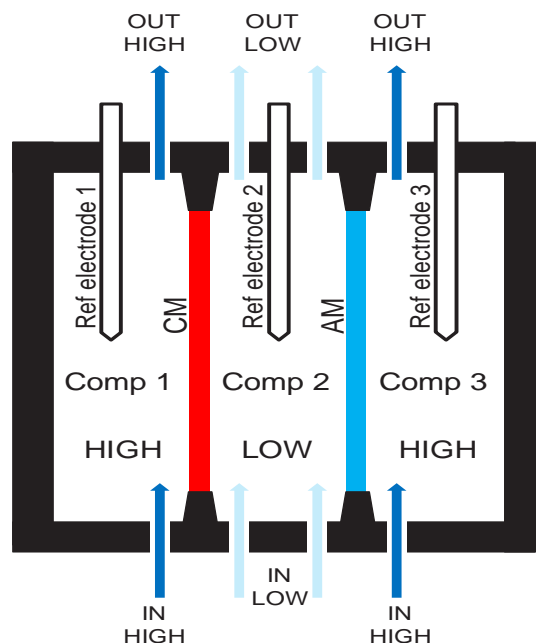
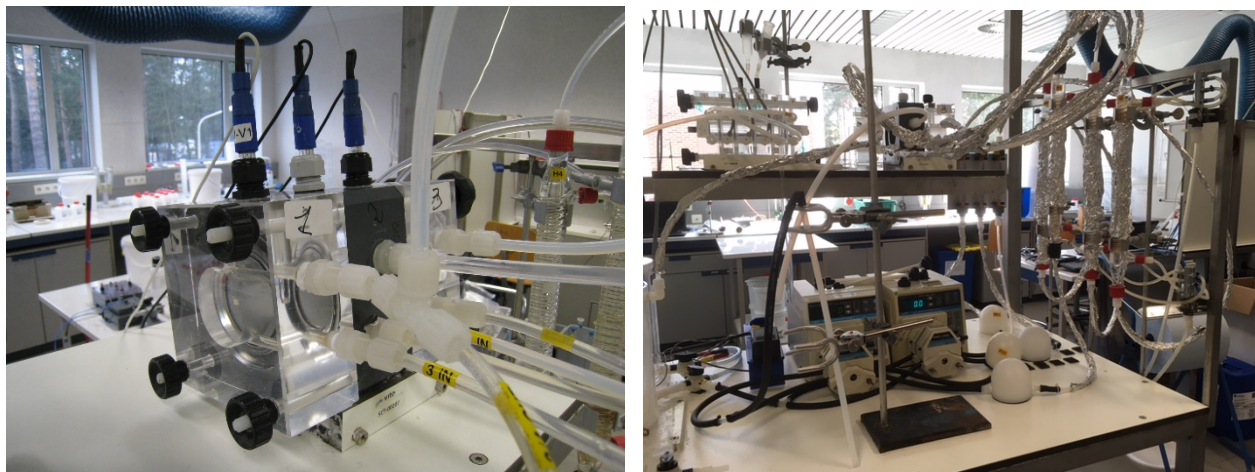


Figure 2 Schematic view of the 3-compartment set-up

In the experiments several concentrations in HIGH and LOW were used; the LOW ranged from 0,1M over 0,05M, to 0,01M, the HIGH from 5M, over 2M to 1M. Also the composition of HIGH was changed by adding Ca and Mg salts. The salinity difference between HIGH and LOW generates an electrochemical potential difference across each of the membranes. For reasons of continued ion transport it is important to have a set-up as shown in Figure 2, consisting of three compartments, the central one being the LOW adjacent to two HIGH compartments. Trying to measure an SGP-RE related ion migration on the basis of a two compartment set-up (as is the case when measuring apparent permselectivity of a single membrane) is not possible and therefore a three compartment set-up is necessary in that perspective. The setup shown in Figure 2, enables the  $\text{Na}^+$  ions to migrate from Compartment1 to Compartment 2 and  $\text{Cl}^-$  ions from Compartment 3 to Compartment 2. Therefore, electro-neutrality is preserved at all times in the three compartments and the transport of ions will continue until both concentrations will be equal. This would be the case where thermodynamic equilibrium is reached when mixing of two salt solutions of different concentrations.

In the set-up a conductivity sensor was integrated in the recycling LOW solution stream as to evaluate the evolution of the LOW concentration, which is increasing in time. The conductivity meter was calibrated by using multiple standard NaCl solutions and by accordingly setting up a conductivity reading versus concentration calibration curve (regression equation). The set-up also included a thermostatic temperature control system in order to keep the temperature of the LOW and HIGH within  $\pm 0.2^\circ\text{C}$  of the set points during the experiment. All readings were logged during the experiments. For the experiments with the multivalent ions samples were taken every 5 minutes- from the LOW and analysed for Ca/Mg content, since conductivity readings cannot reveal the ratio of mono- and bivalent ionic concentration. The flow rates of compartment 1 and 3 was regulated by one peristaltic pump, the flow rate of compartment 2 by a separate one. In Figure 3 pictures of the setup are shown.



*Figure 3 Three-compartment cell and setup including peristaltic pumps and heat exchangers*

Ion transport is always accompanied by transport of water to some extent. Typically a Na-ion for example carries at least 6 water molecules in its so called hydration sphere or shell. When these ions are migrating in the bulk liquid or through a membrane they will therefore also transport water, defined as ‘electroosmotic water transport’. The direction of transport is the same as the transport of the ion, i.e. from HIGH to LOW. The amount of water being transported by electro osmosis depends largely on the salinity difference and the membrane properties. On the other hand water molecules will be transported from LOW to HIGH by osmosis. Due to the concentration difference between LOW and HIGH, an osmotic pressure is exerted in the direction of HIGH, i.e. water molecules will tend to dissolve from the LOW into the membrane and diffuse from the membrane into the HIGH. The osmotic water transport rate is determined largely by the membrane properties and the salinity difference of the solutions. During the experiments the change in volume of the LOW is followed and registered as a flux ( $\text{l/h.m}^2$ ). This number represents the net-flux, as the sum of both electro osmotic and counteracting osmotic water transport. Osmotic water transport tends to be slower than electro osmotic and will therefore be more pronounced during experiments with a long residence time such as the experiments with the 3-compartment setup (typically 1 hour). In a full-blown SGP-RE stack residence times are in approximately 10-30 seconds, in which case the electroosmotic transport will be favoured. In the following calculations the water transport is neglected

### 3.1.3 Data processing

It is assumed that during an experiment a dynamic equilibrium (quasi equilibrium) is present at all times and is defined by the set of two membranes. The individual CM and AM will never show identical intrinsic ion transport rate potential for respectively the cations and anions, i.e. the transport behaviour of cations through the CM and anions through the AM will always differ. Moreover, those membranes will also never be perfectly permselective, nor will they show the same permselectivity. Hence, it can be assumed that the transport of cations from Compartment1 to Compartment2 and the transport of anions from Compartment3 to Compartment2 is self-controlled by a dynamic equilibrium on the basis of the required electro-neutrality in the HIGH and LOW solutions at each time instance of the experiment. Both membranes stay “tuned” in that respect. A relatively slow transport of cations through CM will therefore also slow down the transport of anions through an intrinsically fast AM.

Evidently temperature is an important experimental parameter since it determines the ion flux. The higher the temperature the higher the ion migration rate. Experiments were performed at four temperatures 25 °C, 30 °C, 40 °C, 50 °C and 60 °C. New membranes were mounted for each test, after the typical preconditioning treatment in a salt solution, as required for fresh IEX membranes.

During the experiment the conductivity of the LOW solution (Compartment2) was continuously logged. A data sample was acquired every 10 seconds. Such a sampling rate was adequate, as can be observed from Figure 3. The NaCl concentration was calculated from the conductivity measurements as shown in Figure 4. A second degree polynomial regression is used as equation to relate the measured conductivity during the experiments to the concentration. All conductivity measurements were corrected for a temperature of 25°C.

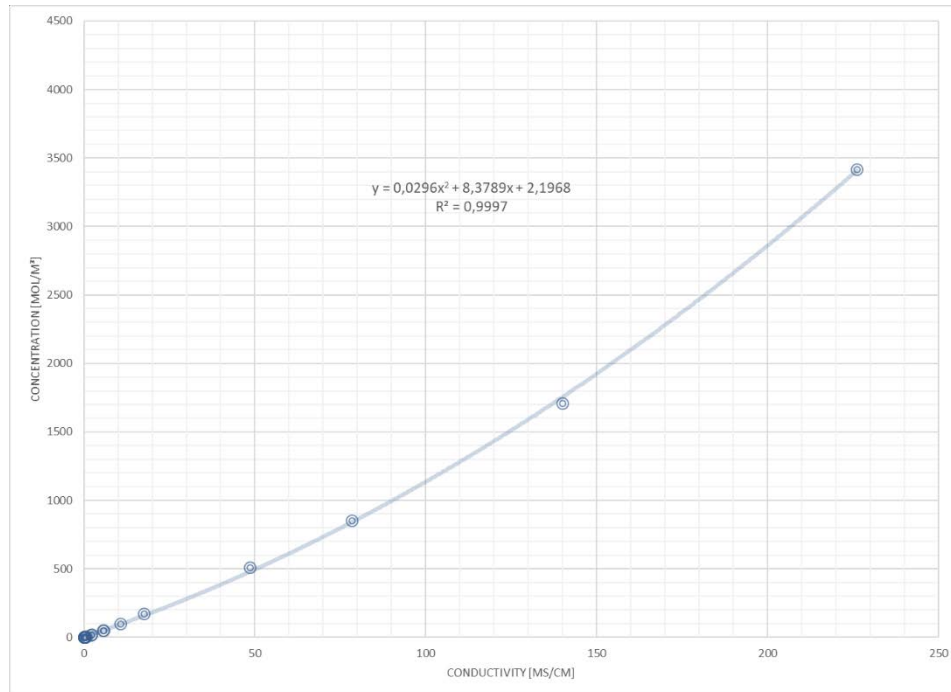


Figure 4 Conductivity vs concentration curve of NaCl solutions (25°C)

The derivative of the second degree regression equation expressing concentration as a function of time ( $\text{conc} = f(t)$ ) can be calculated in order to obtain the value of  $d(\text{conc})/dt$  and therefore also the value of the ionic flux  $J$  ( $\text{mol}/\text{m}^2 \cdot \text{s}$ ). The ionic flux can then be converted into an electrical flux (or current density) by multiplying with Faraday's constant ( $96485\text{C}/\text{mol}$ ). Multiplying the instantaneous measured potential difference with the calculated current density will give the projected power density ( $\text{W}/\text{m}^2$  cell pair)

## 3.2 Results and discussion

### 3.2.1 Experiments with pure NaCl

The first experiments were conducted with pure NaCl solutions at room temperature to check the performance of the selected membranes at different concentrations of HIGH and LOW. In Table 5 the overview of all the experiments with pure NaCl is given. All membrane combinations are tested with the same HIGH and LOW solutions.

Table 5 Overview of experiments with pure NaCl

CEM   AEM   LOW   HIGH (25°C)
FKE20 FAS 20 0,05M NaCl  1M NaCl
FKS20 FAS 20 0,05M NaCl  1M NaCl
FUJI  FUJI  0,05M NaCl  1M NaCl
FKE20 FAS 20 0,05M NaCl  2M NaCl
FKS20 FAS 20 0,05M NaCl  2M NaCl
FUJI  FUJI  0,05M NaCl  2M NaCl
FKE20 FAS 20 0,1M NaCl 2M NaCl
FKS20 FAS 20 0,1M NaCl 2M NaCl
FUJI  FUJI  0,1M NaCl 2M NaCl
FKE20 FAS 20 0,1M NaCl  5M NaCl
FKS20 FAS 20 0,1M NaCl 5M NaCl
FUJI  FUJI  0,1M NaCl 5M NaCl

In Table 6 an overview is given of the half-cell potential measured in each of the experiments. Based on the measured potential in the cell, the apparent permselectivity is calculated as the ratio between the measured and the theoretical Nernst potential (assuming a perfectly selective membrane). The results show that all three membrane pairs perform similar towards the ion-selectivity. The FKS/FAS membrane pair has the highest overall permselectivity and is able to keep this throughout the entire concentration range. The FKE/FAS couple has a slightly decreased permselectivity at 0,1M|2M and 0,1M|5M, which is a bit counterintuitive as can be expected the permselectivity would decrease with increasing concentrations and concentration differences. The FUJI membranes are performing best in the 2M range and less at concentrations of 1M and 5M. Again, the latter is unexpected, although the differences in are minor overall.

Table 6 Pure NaCl experiments: overview of half-cell potential and apparent permselectivity

full name	half-cell potential (mV)	Apparent permselectivity(*)
FKE20 FAS 20 0,05M NaCl  1M NaCl	66	0,86
FKS20 FAS 20 0,05M NaCl  1M NaCl	66	0,86
FUJI  FUJI  0,05M NaCl  1M NaCl	56	0,73
FKE20 FAS 20 0,05M NaCl  2M NaCl	80	0,84
FKS20 FAS 20 0,05M NaCl  2M NaCl	79	0,83
FUJI  FUJI  0,05M NaCl  2M NaCl	76	0,80
FKE20 FAS 20 0,1M NaCl 2M NaCl	61	0,79
FKS20 FAS 20 0,1M NaCl 2M NaCl	64	0,83
FUJI  FUJI  0,1M NaCl 2M NaCl	62	0,81



full name	half-cell potential (mV)	Apparent permselectivity(*)
FKE20 FAS 20 0,1M NaCl  5M NaCl	79	0,79
FKS20 FAS 20 0,1M NaCl  5M NaCl	83	0,83
FUJI  FUJI  0,1M NaCl 5M NaCl	75	0,75

(\*) calculated as the ratio of the measured half-cell potential (mean value of AEM and CEM) and the theoretical Nernst potential

Figure 5 gives the results of the experiments in terms of power density and current density of the FUJI membranes. As expected the highest power density was obtained with the largest concentration difference between HIGH and LOW. When lowering the HIGH concentration to 2M the power density decreases significantly due to the lower gradient.

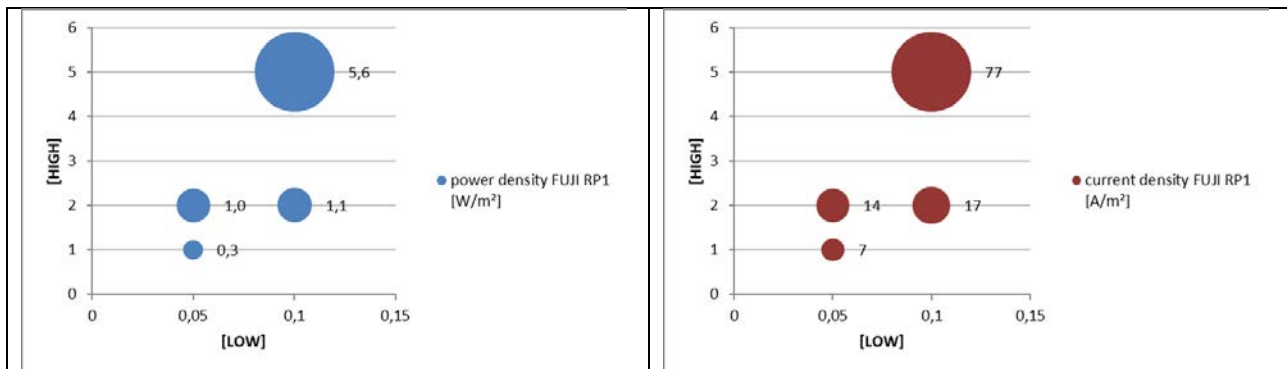


Figure 5 Power density (left) and current density (right) as a function of the concentration of HIGH and LOW for FUJI membranes

It is also clear from Figure 5 that the current density follow the same trend: higher concentration differences translate in higher current densities. This is due partly to the increased cell potential, partly to the increased conductivity of the HIGH and LOW.

In Figure 6 the power and current density data are given for the FKE/FAS membranes. The first thing to notice is the lower power density at high concentrations (5M) which is observed, compared to the FUJI membranes. On the other hand the FKE/FAS combination does not seem to be affected much by the decrease of the HIGH concentration. The remaining power density at 2M (HIGH) is significantly higher than in the case with the FUJI membranes. Similar observations apply for the current density.

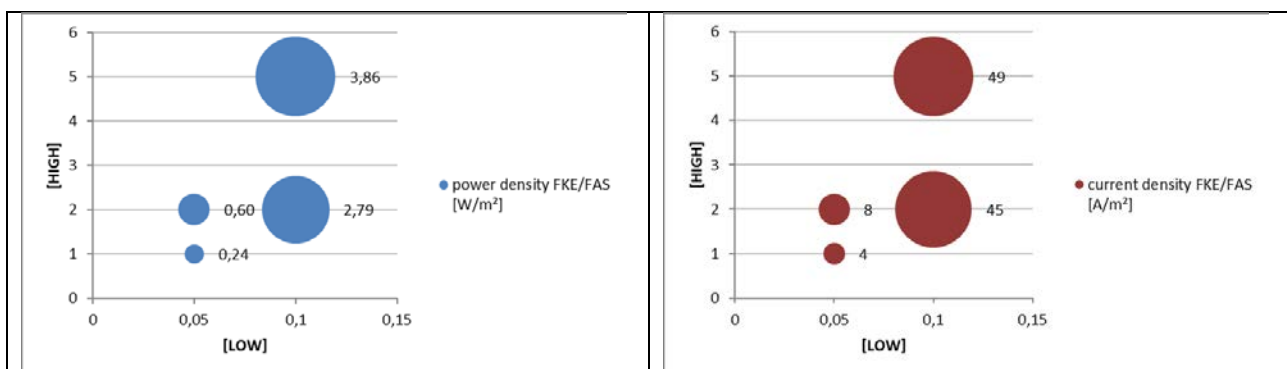


Figure 6 Power density (left) and current density (right) as a function of the concentration of HIGH and LOW for FKE/FAS membranes

For the FKS/FAS membrane pair the results are significantly lower than the prior two membrane pairs in the high concentration ranges. At 2M and 1M HIGH the results are comparable or even better than the first two membrane pairs. Remarkable in this case is the steady power output at 2M HIGH when the LOW concentration drops from 0,1 tot 0,05M. Both power output and current density remain at approximately the same level.

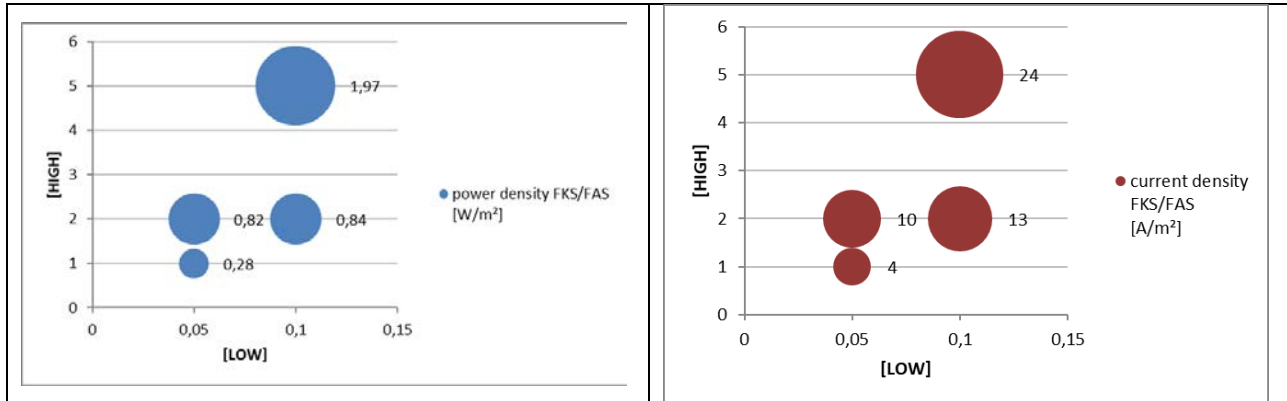


Figure 7 Power density (left) and current density (right) as a function of the concentration of HIGH and LOW for FKS/FAS membranes

Overall the following conclusions can be drawn from this set of experiments with pure NaCl solutions:

- All membrane pairs have a specific optimal range for operation. The FKE/FAS pair works best at 2M vs 0,1M, the FUJI membranes at 5M vs 0,1M, the FKS/FAS couple at 2M vs 0,05M
- Permselectivity of all membranes is high and very consistent throughout the entire concentration range that was selected.

Because of these reasons two membrane pairs were selected for the next set of experiments, including multivalent ions: FUJI and FKE/FAS. The small differences in performance could not be used as a criterion for exclusion from the remaining tests.

### 3.2.2 Experiments at increased temperature

A third set of experiments was conducted to check the performance of the two selected membrane pairs at elevated temperatures. LOW was invariably a pure NaCl solution of 0,1M, HIGH a pure NaCl solution of 2M. In Table 8 the overview of all the experiments and the conditions at increased temperature is given.

Table 7 Overview of experiments at increased temperature

CEM   AEM   LOW   HIGH (25°C)	temperature
FKE20   FAS 20   0,01M NaCl   2M NaCl	25,00
FKE20   FAS 20   0,01M NaCl   2M NaCl	30,00
FKE20   FAS 20   0,01M NaCl   2M NaCl	40,00
FKE20   FAS 20   0,01M NaCl   2M NaCl	50,00
FKE20   FAS 20   0,01M NaCl   2M NaCl	60,00
FUJI   FUJI   0,01M NaCl   2M NaCl	25,00
FUJI   FUJI   0,01M NaCl   2M NaCl	30,00
FUJI   FUJI   0,01M NaCl   2M NaCl	40,00
FUJI   FUJI   0,01M NaCl   2M NaCl	50,00
FUJI   FUJI   0,01M NaCl   2M NaCl	60,00

In Figure 8 the results for the FKE/FAS membrane pair are shown in terms of half-cell potential and apparent permselectivity. Although theoretically the cell potential increases proportionally to the temperature, it can be seen that the measured half-cell potential is decreasing at higher temperature.

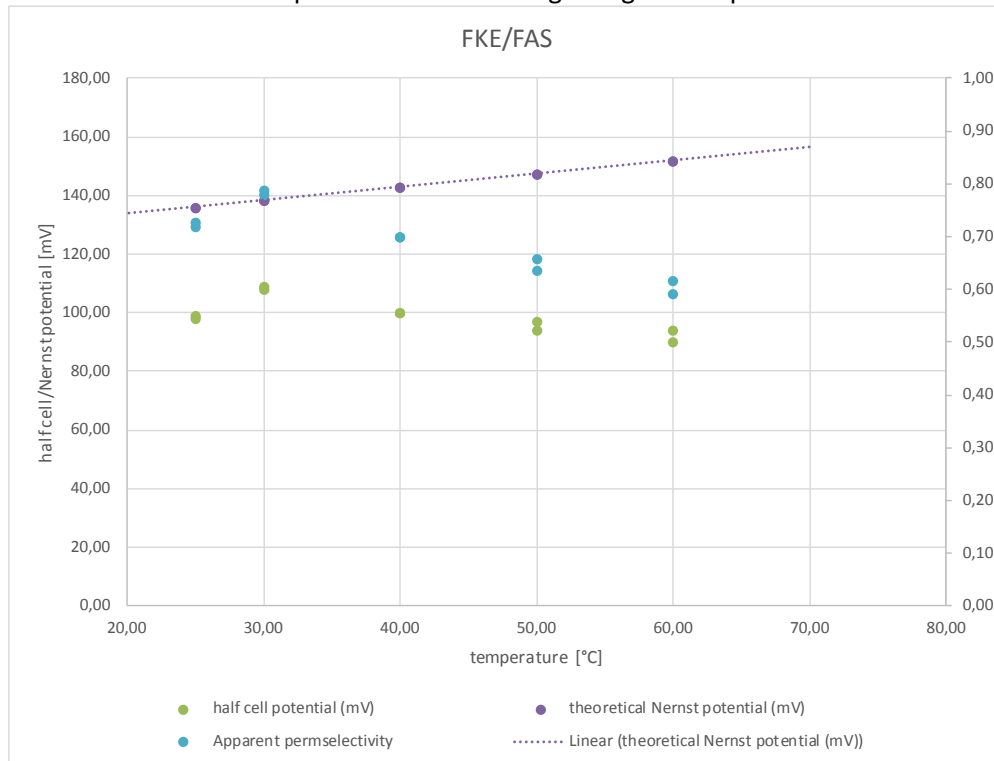
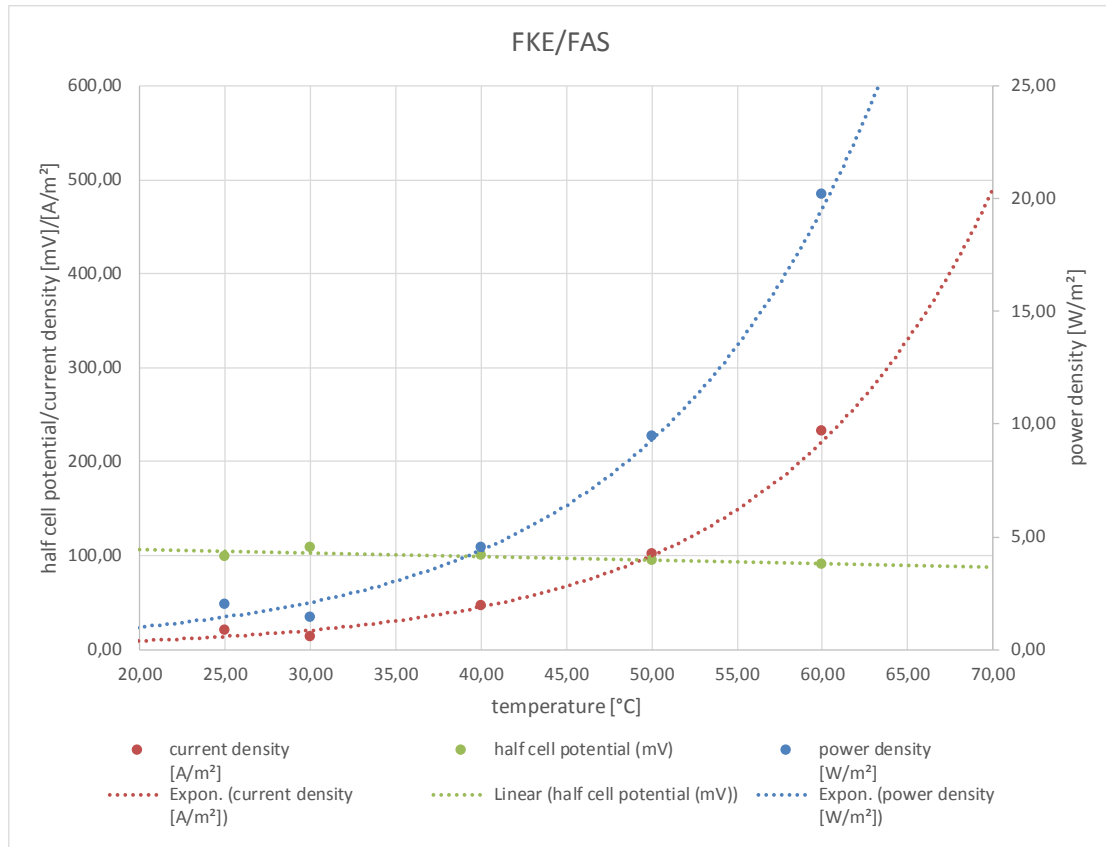


Figure 8 FKE/FAS @ increased temperature half-cell potential and permselectivity

This can be explained by the permselectivity of the ion exchange membrane that is declining with increasing temperatures. At room temperature the membrane would be able to pass easily the counter-ions and retain the co-ions. However as the temperature of the bulk liquid and the membrane rises, also the mobility of the ions (both counter- and co-ions) is increased in the liquid and in the membrane. The initially slow transport of co-ions through the membrane will now be favored by the increasing temperature, relatively more than the transport of counter-ions. This will result in a loss of permselectivity. So the intrinsic increase of the Nernst potential is counteracted by the loss in permselectivity of the membrane. The extent to which membranes are prone to loss of permselectivity is depending on the type of membrane (heterogeneous/homogeneous/charge density) and the thickness. It plays a very important role in the application of SGP-RE for energy extraction of geothermal brine since most brines have a temperature warmer than 30-40°C. In the case of the FKE/FAS membranes the decline of the permselectivity already starts at 30°C.



*Figure 9 FKE/FAS @ increased temperature: power and current density results*

Figure 9 gives the power and current density for the same membrane pair (FKE/FAS). Both the current density and the power density increase exponentially with increasing temperature. It is obvious that the small decrease in half-cell potential is overcompensated by the exponential increase in the current density. Compared to 25°C, the power output is a ten-fold higher at 60°C. This is one of the most beneficial effects of working with geothermal brines.



Figure 10 shows the results for the FUJI membrane pair in terms of half-cell potential and apparent permselectivity. In this case the apparent permselectivity is decreasing starting from 25°C, although the decrease is less than in the case of the FKE/FAS. The measured half-cell potential is almost constant over the entire temperature range from 25-60°C. It can be concluded that the FUJI membranes are more resistant in terms of selectivity to a temperature increase. The membranes are 6 times thicker than the FKE/FAS membranes and therefore intrinsically more resistant to loss of permselectivity at higher temperatures, since the polymeric ion-exchange barrier is simply more extended.

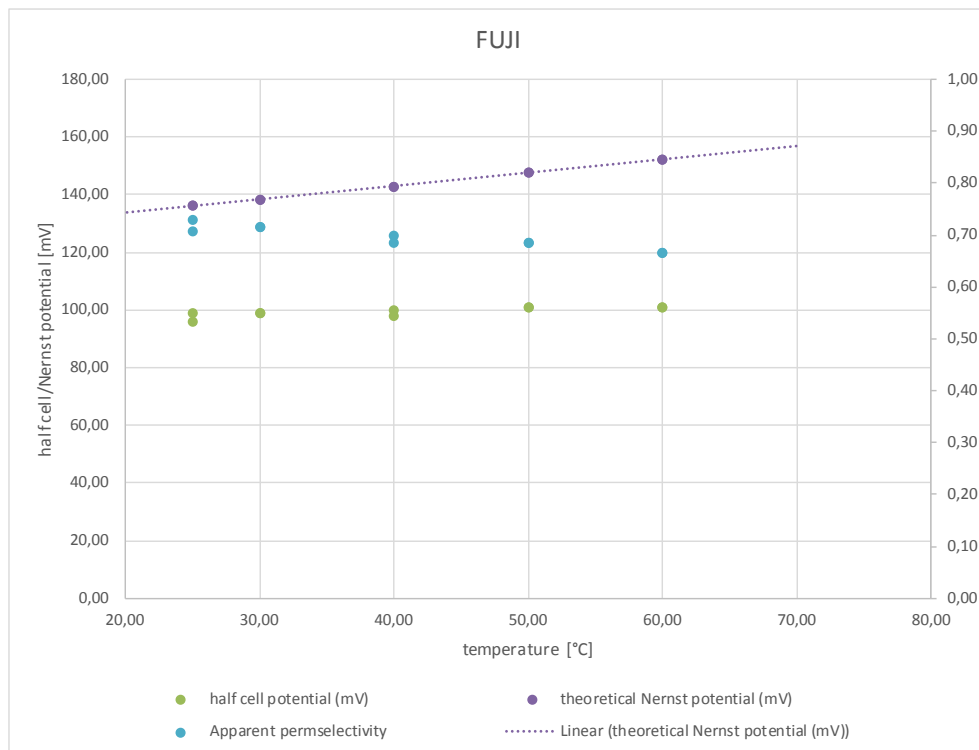
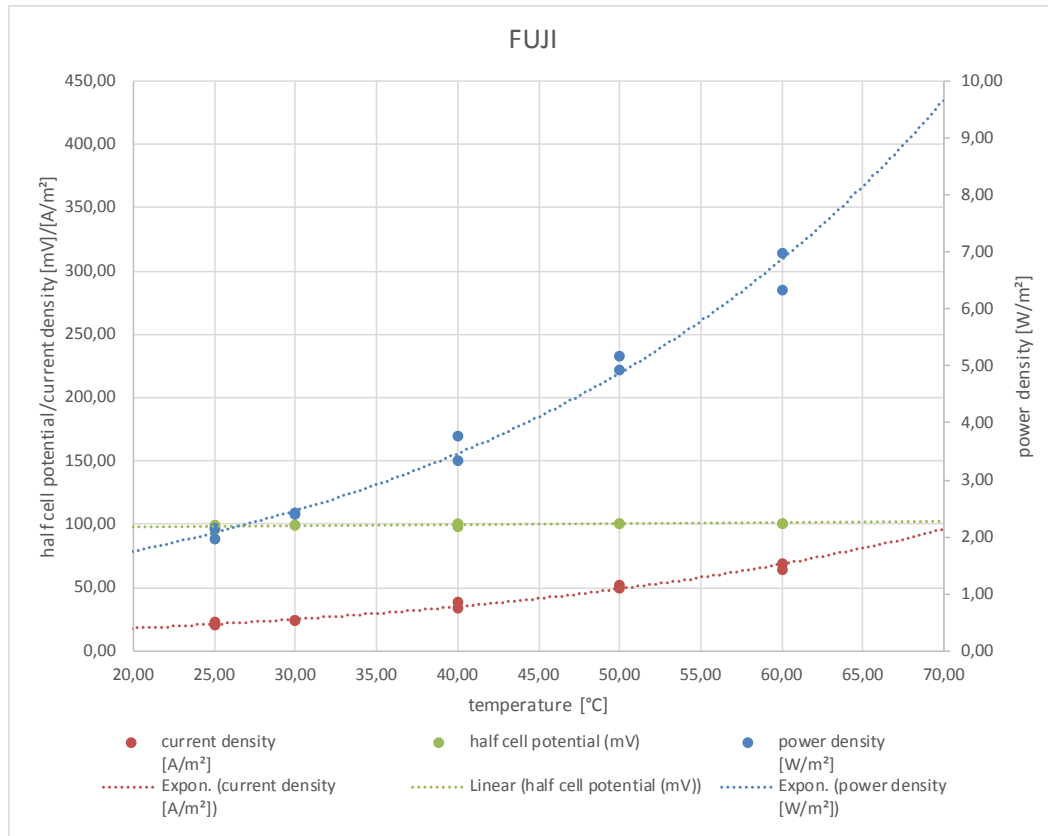


Figure 10 FUJI @ increased temperature: half-cell potential and permselectivity results

Figure 11 Figure 9 gives the power and current density for the FUJI membranes. A similar trend as with the FKE/FAS membranes is observed: both current and power density are increasing exponentially with the temperature. Although in this case the increase is far less than in the previous case, where a 10 times increase in power density occurred. With the FUJI membranes the power density is increased little more than three times the value at 25°C. As in the previous, also here the current density is causing this increase and from the graph it is obvious that current density is not equally affected by temperature as clearly demonstrated in Figure 9. It can thus be concluded that the membranes have less benefit -at least in terms of power output- of being used at higher temperatures.



*Figure 11 FUJI@ increased temperature power and current density results*

It can be concluded that the temperature has a very substantial positive effect of the performance of the SGP-RE cell pair. It was demonstrated that increasing the temperature to 60°C resulted in a 10-fold increase of the power density, based on a single cell pair. A fundamental correlation between the membrane thickness (and type) and the temperature dependency of the performance was revealed. Clearly, thin, homogenous membranes are benefitting more from operating at higher temperatures. This information is very valuable for the actual implementation and design of a larger scale SGP-RE plant.

### 3.2.3 Experiments with multivalent ions

The second set of experiments was conducted with a mixture of NaCl, CaCl<sub>2</sub> and MgCl<sub>2</sub> solutions at room temperature to check the performance of the selected membranes at different concentrations of the multivalent ions. LOW was invariably a pure NaCl solution of 0,1M. The HIGH composition varied, but the cation molarity always added to 5M. Different concentration ranges for the Mg and Ca were used with the FUJI membranes, for the FKE/FAS membranes on CA was tested. In Table 8 the overview of all the experiments with multivalent salts is given. Besides the tests with multivalent ions also a reference test with 5M NaCl vs 0,1M NaCl was carried out for both membrane pairs.

*Table 8 Overview of experiments with multivalent ions*

CEM   AEM   LOW   HIGH (25°C)	
Subset 1	
FUJI   FUJI	0,1M NaCl   4,75M NaCl - 0,25M CaCl <sub>2</sub>
FUJI   FUJI	0,1M NaCl   4,9M NaCl - 0,1M CaCl <sub>2</sub>
FUJI   FUJI	0,1M NaCl   4,99M NaCl - 0,01M CaCl <sub>2</sub>
FUJI   FUJI	0,1M NaCl   4,75M NaCl - 0,25M MgCl <sub>2</sub>
FUJI   FUJI	0,1M NaCl   4,9M NaCl - 0,1M MgCl <sub>2</sub>
FUJI   FUJI	0,1M NaCl   4,99M NaCl - 0,01M MgCl <sub>2</sub>
FKE20   FAS 20	0,1M NaCl   4,75M NaCl - 0,25M CaCl <sub>2</sub>
FKE20   FAS 20	0,1M NaCl   4,9M NaCl - 0,1M CaCl <sub>2</sub>
FKE20   FAS 20	0,1M NaCl   4,99M NaCl - 0,01M CaCl <sub>2</sub>

In Figure 12 the power- and current density and the half-cell potential are given for the experiments with the FUJI membranes. The first bars shows the result for a 5M HIGH solution vs 0,1M LOW. This test was performed just before the rest of the experiments as a benchmark. The results show that the cell potential is not affected much by the presence of multivalent ions. The reason is that the total molarity of the solutions throughout all the tests is the same for the cations. In terms of current density it can be concluded that presence of Mg has a negative effect, although not very pronounced. The presence of Ca seems to have a slightly positive effect in moderate to low concentrations. This is also reflected in a slightly higher power density. Overall the effects of Ca and Mg in these tests remain very limited and even within error margin of the test output.

Because of the positive effect of Ca with the FUJI membranes another set of experiments was conducted with Ca, this time with the FKE/FAS membranes. The results in Figure 13 show that Ca also enhance the current- and power density for these membranes. The cell potential remained -as previously observed- unchanged. The effects of Ca remain even for this membrane pair very limited, almost insignificant.

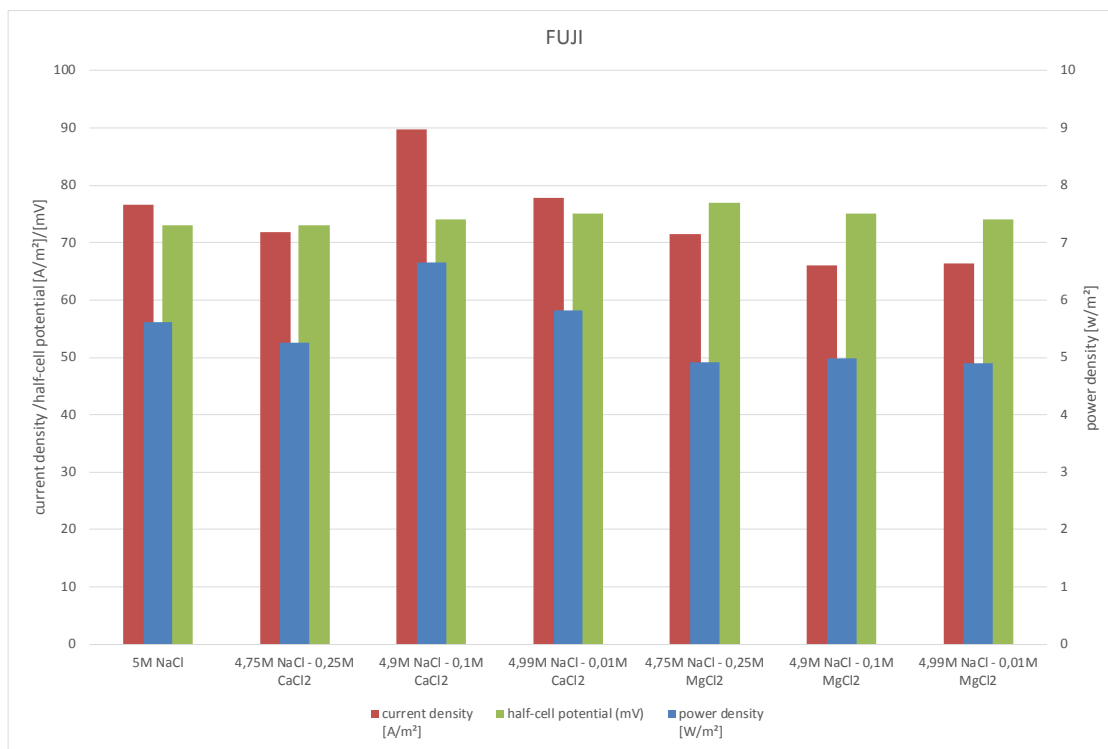


Figure 12 Experimental results FUJI membranes: influence of Ca and Mg

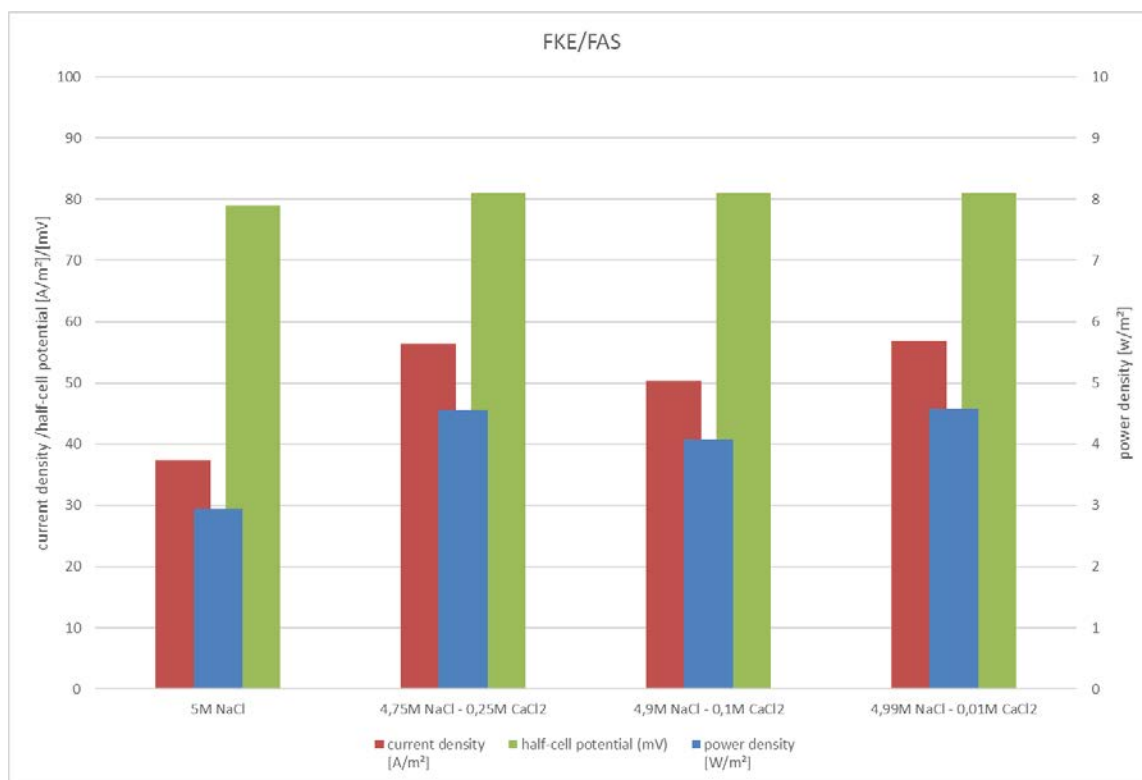


Figure 13 Experimental results FKS/FAS membranes: influence of Ca and Mg

### 3.2.4 Experiments with multivalent ion combinations at increased temperature

The final set of experiments with the 3-compartment setup consisted of a combined parameter experiment, where the presence of multivalent ions (Ca and Mg) and the temperature dependence were evaluated at the same time. The overview of the experiments is given in Table 9. This set of experiments should be combined and compared with the experiments in Table 7

Table 9 Overview of experiments with multivalent ions at increased temperature

CEM   AEM   LOW   HIGH	Temperature (°C)
FKE20 FAS 20 0,01M NaCl 1,5M NaCl - 0,25M CaCl <sub>2</sub> - 0,05M MgCl <sub>2</sub>	25
FKE20 FAS 20 0,01M NaCl 1,5M NaCl - 0,25M CaCl <sub>2</sub> - 0,05M MgCl <sub>2</sub>	30
FKE20 FAS 20 0,01M NaCl 1,5M NaCl - 0,25M CaCl <sub>2</sub> - 0,05M MgCl <sub>2</sub>	40
FKE20 FAS 20 0,01M NaCl 1,5M NaCl - 0,25M CaCl <sub>2</sub> - 0,05M MgCl <sub>2</sub>	50
FKE20 FAS 20 0,01M NaCl 1,5M NaCl - 0,25M CaCl <sub>2</sub> - 0,05M MgCl <sub>2</sub>	60

The results can be found in Figure 14. The half-cell potential is more or less steady except at 25°C, where it drops to almost half the value for unclear reasons. Possibly a leakage between the compartments could have caused this. A slight decrease in cell potential can also be seen at 50 and 60°C. The current- and power density follow the expected exponential trend as in section 3.2.2, however the absolute values are much lower than previously observed (cf. Figure 15 for comparison).

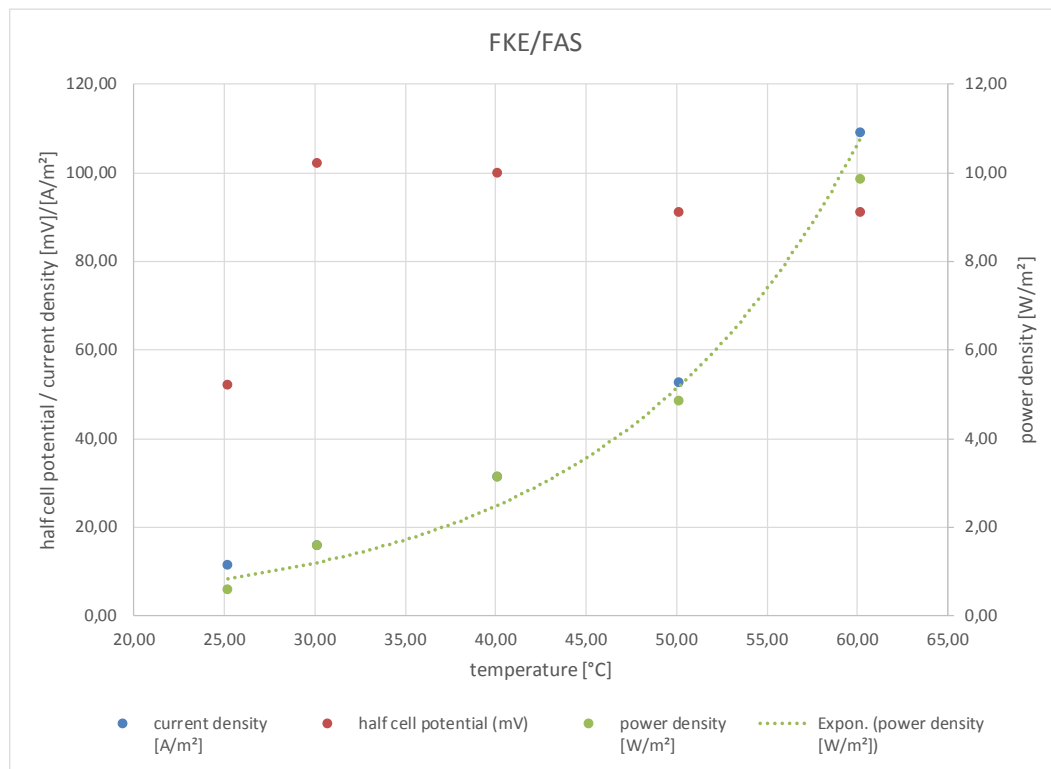


Figure 14 Experimental results of combined test (Ca+Mg) with FKE/FAS: current- and power density as a function of temperature

In Figure 15 the results of the combined test (Ca+Mg) are compared with the results from section 3.2.2. In this graph the effect of the Ca and Mg on the performance of the single cell is very clear. Although no decrease was observed at 30°C this could be due to an erroneous measurement. In terms of cell potential the addition of Ca and Mg shows no negative effects. The main effect of Ca and Mg is on the current density and power

density, both are reduced significantly by the presence of Ca and Mg. The decrease is consistent throughout the entire temperature range.

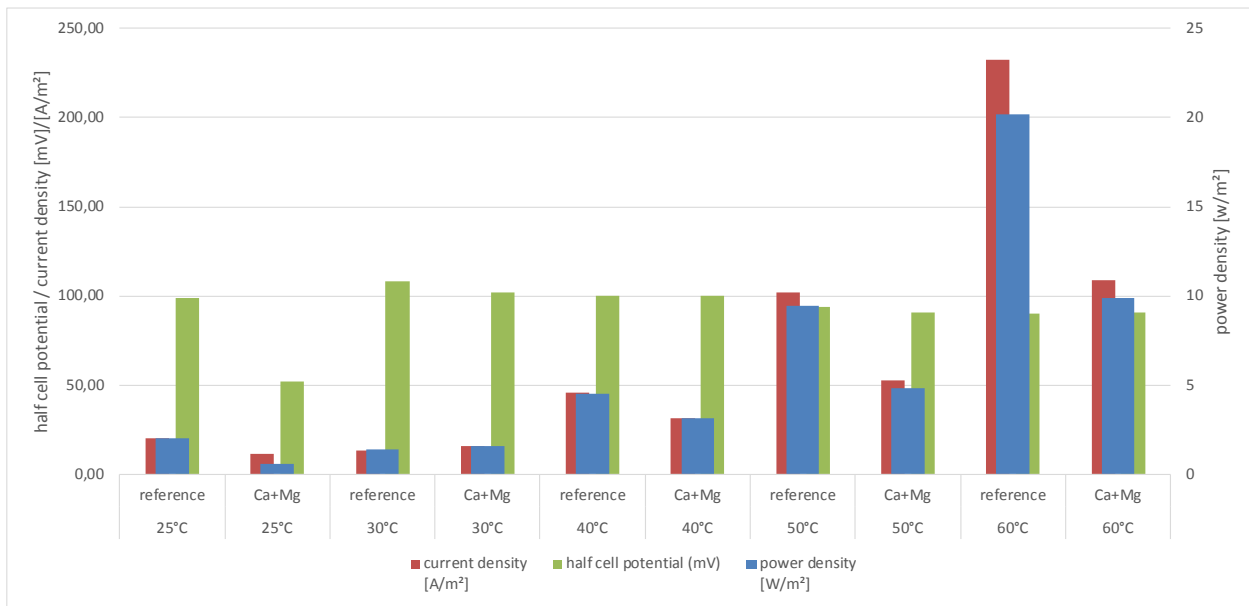


Figure 15 Comparison of reference test results and combined test (Ca+Mg) with FKE/FAS: current- and power density as a function of temperature



## 4 Pilot scale experiments

### 4.1 Materials and methods

The pilot system was conceived in a similar way as traditional electrodialysis systems, consisting of three separate loops with almost identical instrumentation and a common control system. In Figure 16 the instrumentation side of the pilot plant is shown, clearly visible are the (blue) centrifugal and (yellow) peristaltic pumps of each loop: LOW, HIGH and ELEC from left to right.

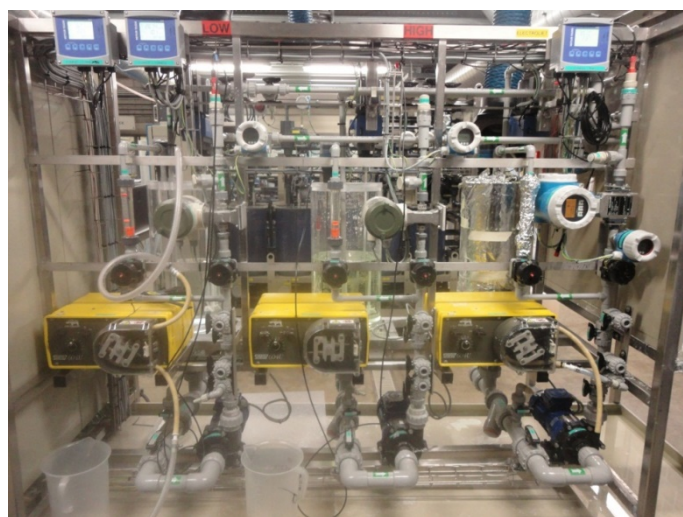


Figure 16 SGP-RE pilot plant: instrumentation side

In Figure 17 the other side of the installation is shown with the three buffer tanks (ELEC buffer tank covered with aluminum foil to prevent degradation of electrolyte under influence of UV light). For reasons of confidentiality a picture of the SGP-RE stack itself cannot be shown.

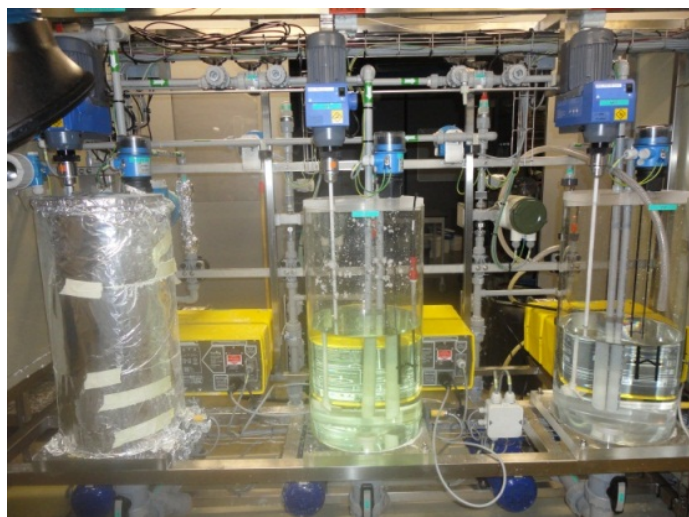


Figure 17 SGP-RE pilot plant: tank side (ELEC, HIGH, LOW, from left to right)

The LOW and HIGH circulation loop are identical and consist each of:

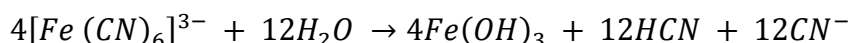
- Polycarbonate transparent buffer tank of 30L equipped with a vertical stirrer, low level sensor and pressure measurement for measuring liquid level in tank.
- In-line filter 500µm for protection of pumps
- centrifugal pump: Iwaki magnetically coupled pump MDH-400CV5-D

- peristaltic pump: WATSON MARLOW©604U
- By-pass system with rotameter flow reading to reduce flow to stack
- Flow measurement: Yokogawa AE105MG 08FT1.010
- Conductivity and temperature measurement on inlet of stack: Mettler Toledo
- Pressure measurement on inlet of stack
- Pressure measurement on outlet of stack
- Conductivity and temperature measurement on outlet of stack: Mettler Toledo

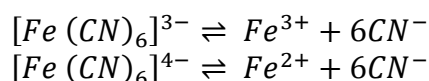
The ELEC circulation loop consists of:

- Polycarbonate transparent buffer tank of 30L equipped with a vertical stirrer, low level sensor and pressure measurement for measuring liquid level in tank.
- In-line filter 500µm for protection of pumps
- centrifugal pump: Iwaki pump MDH-400CV5-D
- peristaltic pump: Watson-Marlow
- By-pass system with rotameter flow reading to reduce flow to stack
- Flow measurement: Yokogawa AE105MG 08FT1.010
- Conductivity and temperature measurement on inlet of stack: Mettler Toledo
- Pressure measurement on inlet of stack
- Conductivity and temperature measurement on outlet of stack: Mettler Toledo
- pH measurement KNICK Inpro 4850i

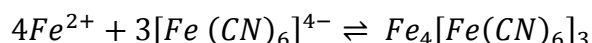
For SGP-RE process the selection of an appropriate redox couple is essential, in order to convert the ionic current into an electric current via an external electrical circuit. From prior experience  $K_3Fe(CN)_6 / K_4Fe(CN)_6 \cdot 3H_2O$  was selected as a redox couple. The presence of the CN<sup>-</sup> ligand that complex the iron ions makes this redox couple stable in a wide pH range. However, the  $K_3Fe(CN)_6 / K_4Fe(CN)_6 \cdot 3H_2O$  have to be used in absence of molecular oxygen (radicals) and light. Sunlight activates the formation of the cyanide ion, toxic, according to the following reaction:



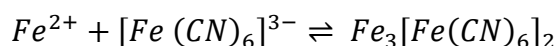
It's been estimated that in the presence of air but in the absence of light, the ferrocyanide is converted completely into ferricyanide in 100 days at pH 7. In the presence of sunlight ferrocyanide decomposes with formation of cyanide ions as a result. Also acidification promotes the decomposition of the cyanide complex according to :



In this way a intermediate product, so-called Prussian blue is formed:



and also the Turnbull blue:



Besides degradation of the electrolyte rinse solution, also leakage or diffusion from the ELEC to HIGH or LOW should be prevented. In order to achieve this, two external Nafion 117membranes are used as end membranes, covering the electrodes. They are cationic exchange membranes, and therefore prevent the passage of the cyanide complex (negatively charged) from the electrode compartments to the adjacent ones and they are designed to work in the presence of high concentrations of NaCl.

All input signals are collected via field point modules (National Instruments) and are recorded and processed via the LabVIEW® (Laboratory Virtual Instrumentation Engineering Workbench – National Instruments) software (designed by VITO, called MeFiAS<sup>1</sup>). VITO specifically adapted the core of the system to match the requirements of this application.

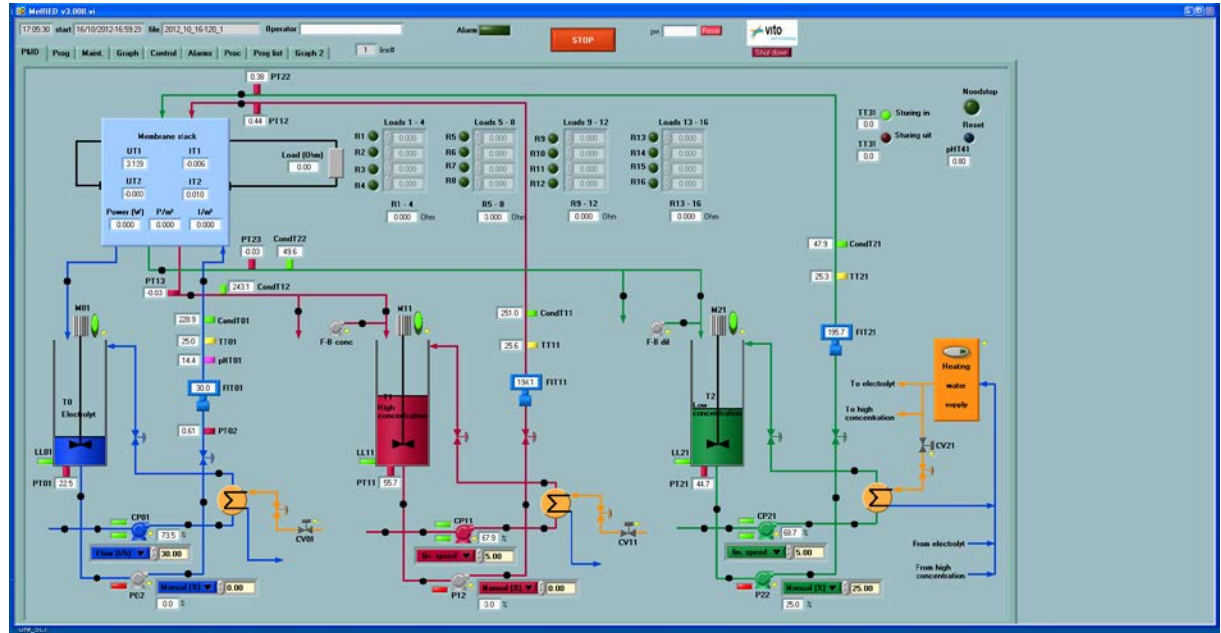


Figure 18 Screen shot of MeFiAS software

So called program Lines can be defined in Mefias and are used for switching on or off of equipment (pumps, valves, stirrers), control flow rates or linear velocity of the solutions inside each channel of the stack, control rules of process parameters; alarms and the stop systems of the pilot plant and duration of the control program.

The different program lines can be saved and imported into the control window *Program*. From this window all the characteristics of the stack are set: membrane size, number of cell pairs, thickness of the spacer, relative volume of the spacer compared to the one of the channel. These properties are used to calculate the average linear velocity of the two solutions within the channels. In particular, the average linear velocity is equal to:

$$v = \frac{\dot{Q}}{S_{free}}$$

$\dot{Q}$  is the flow rate and  $S_{free}$  the free surface. The free surface is related to the free volume within the channel:

$$V_{free} = V_C - V_S$$

$$V_{free} = V_C - 0,175 \cdot V_C$$

$$V_{free} = w_c \cdot l_c \cdot t_c - 0,175 \cdot w_c \cdot l_c \cdot t_c \cdot t_c(1 - 0,175)$$

<sup>1</sup> MeFiAS: Membrane Filtration Acquisition system

$V_{free}$  is the free volume,  $V_c$  is the volume of the channel,  $V_s$  is the volume of the spacer,  $w_c$  is the width of the channel,  $l$  the length,  $t$  the thickness. The percentage of volume occupied by the spacer is equal to 17,5%. The free surface is equal to the free volume divided by the length:

$$S_{free} = w_c \cdot t_c (1 - 0,175)$$

So the linear velocity is equal to:

$$v = \frac{\dot{Q}}{S_{free}} = \frac{\dot{Q}}{w_c \cdot t_c (1 - 0,175)}$$

$w_c = 10\text{cm}$  and  $t_c = 270 \mu\text{m}$ .

The experimental tests are been performed connecting the stack to a galvanostat (AMEL 2044). Before performing the experiments, it is necessary for the system to reach a stable condition (concentrations, stack voltage, flow rates etc.)

Power measurements are performed by applying a fixed current (galvanostatic control mode) from 0mA to 1000mA in steps of 50mA and measuring the voltage response of the stack. The electrodes of the stack are connected to the acquisition system to monitor continuously the electrical variables (current  $I$  [A], difference in potential between the electrodes  $\Delta V$  [V]) related by the following relationship

$$\Delta V = OCV - R_{stack} \cdot I$$

The OCV, is the difference in potential between the electrodes in the absence of current circulation,  $R_{stack}$  [ $\Omega$ ] is the electrical resistance of the stack. In a graph potential vs. current the OCV is the intercept of the straight line with the potential axis,  $I_{shortcut}$  (shortcut current) is the intercept with the current axis and  $R_{stack}$  is the slope.

The electric power  $P$  [W] is equal to the product of the current  $I$  [A] and the difference in potential  $\Delta V$  [V]:

$$P = \Delta V \cdot I$$

It's possible to normalize the electric power respect to the total area of the membranes obtaining the power density:

$$P_d = \frac{P}{N_{cell\ pairs} \cdot A}$$

$P_d$  is the power density [ $\text{W}/\text{m}^2$ ],  $P$  is the electric power [W],  $N_{cell\ pairs}$  is the number of cell pairs and  $A$  is the active surface of an ionic exchange membrane [ $\text{m}^2$ ].

The net power density  $P_{density\_Net}$  [ $\text{W}/\text{m}^2$ ] is equal to the difference between the electric power  $P$  [W] and the power required for pumping the fluids, divided by the total surface of the membranes:

$$P_{density\_Net} = \frac{P - \Delta p_{High} \dot{Q}_{High} - \Delta p_{low} \dot{Q}_{low}}{A_{Tot}}$$

$\Delta p_{High}$  and  $\Delta p_{low}$  are the pressure drops calculated by the pressure transmitters as the difference in pressure between the inlet and the outlet of the stack,  $\dot{Q}_{High}$  and  $\dot{Q}_{low}$  are the flow rates, corresponding to HIGH and LOW,  $A_{tot}$  is the active surface of a membrane multiplying by the number of cell pairs.

After completion of a series of experiments the electrode rinse solution is removed from the external compartment of the stack and the stack is then rinsed and filled with a 2M NaCl solution, waiting for the next set of experiments.

Testing of the SGP-RE stack is done in galvanostatic mode, i.e. the stack voltage is measured at different values of a current that is imposed on to the stack. Figure 7 gives an example of the results of such a measurement.

Fitting the experimental points of Figure 7, is possible to obtain a straight line according to Equation 8.  $I$  is the current which is set,  $\Delta V$  is the measured difference in voltage, the OCV (Open Circuit Voltage) is the intercept with the voltage axis,  $I_{\text{shortcut}}$  (shortcut current) is the intercept with the current axis,  $R_{\text{stack}}$  (stack resistance) is the slope of the straight line.

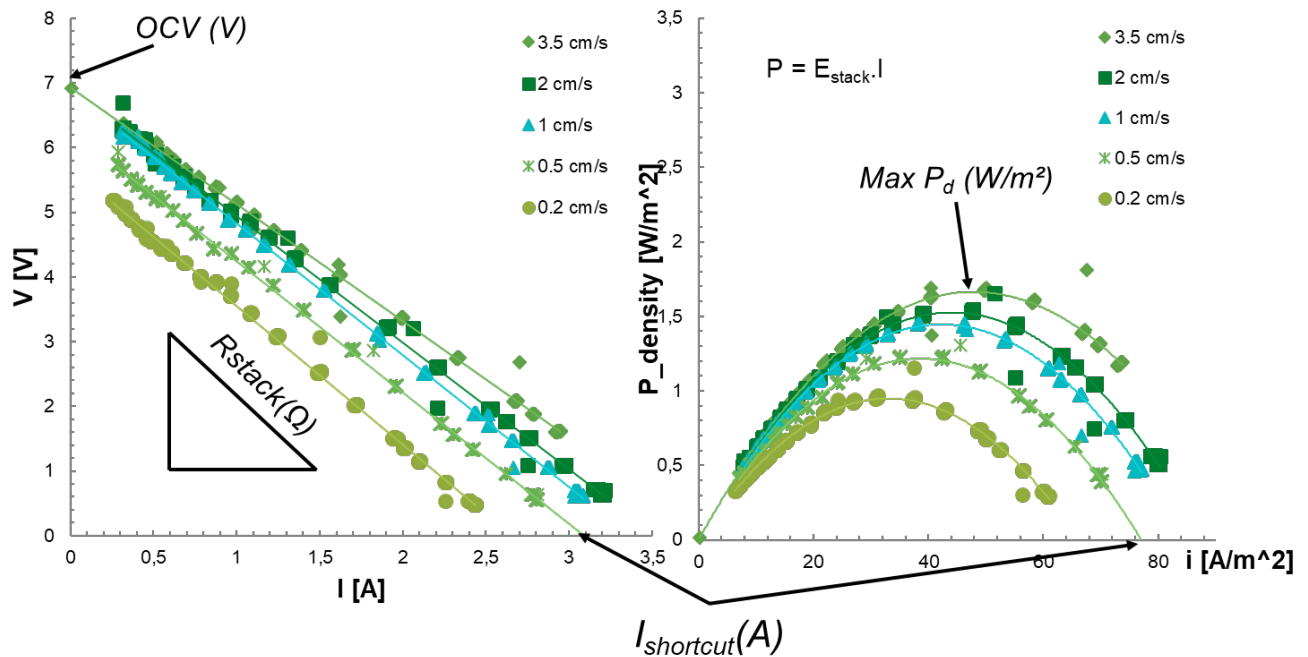


Figure 19 Typical Voltage-current and power density-current density graphs during galvanostatic experiments

The electric power is equal to the current multiplied by the voltage. It is possible to normalize the electric power with respect to the cell pair area, obtaining the power density [ $\text{W}/\text{m}^2$ ].

Increasing the current the voltage decreases, so in two conditions the electric power equals zero, the first one when the current is zero (open circuit), the second one when the voltage is equal to zero (shortcut). The power is the product of the current and the voltage, both positive, so also the electric power is positive. The power density curve is a concave down parabola with two zero points and a maximum point.

In Figure 8 is plotted the power density vs. the current density (current divided by the activated surface of a membrane). Each parabola is described by an equation like the following one:

$$P_{\text{density}} = -a \cdot i^2 + b \cdot i$$

$i$  is the current density [ $\text{W}/\text{m}^2$ ],  $a$  and  $b$  are two parameters obtained by the fitting of the experimental data of Figure 19.. Deriving the above equation and setting the derivative equal to zero:

$$\frac{dP_{\text{density}}}{di} = -2 \cdot a \cdot i + b = 0$$

This way it is possible to obtain the current density  $i_P \text{ Max}$  corresponding to the maximum power density:

$$i_{PMax} = \frac{b}{2a}$$

For SGP-RE process the net power is an important parameter, i.e. the generated energy minus the energy needed for pumping the fluids. In order to obtain a net positive value for the power output, the energy required for pumping the fluids has to be lower than the energy produced by the system.

Net power density can be defined as:

$$P_{density\_Net} = \frac{P - \Delta p_{High} \dot{Q}_{High} - \Delta p_{low} \dot{Q}_{low}}{A_{Tot}}$$

$P_{density\_Net}$  is the net power density,  $\Delta p_{High}$  and  $\Delta p_{low}$  are the pressure drops,  $\dot{Q}_{High}$  and  $\dot{Q}_{low}$  the flow rates of respectively HIGH and LOW.

The main parameters under investigation during the testing of the lab-scale stack were *temperature* and *composition* of the HIGH/LOW. In order to evaluate the effect of these parameters on the performance of the stack a set of reference conditions was defined (Table 10). The reference tests were carried out at 25°C and 50°C. Before and after each test, the stack was triple-tested at the reference conditions.

Table 10 Reference conditions (25°C and 50°C)

ELEC	concentration [M]	Flow rate [l/h]
<b>K<sub>3</sub>Fe(CN)<sub>6</sub></b>	0,3	30
<b>K<sub>4</sub>Fe(CN)<sub>6</sub> · 3H<sub>2</sub>O</b>	0,1	
<b>NaCl</b>	1,5	
Salt solution	concentration [M]	Linear speed [cm/s]
<b>HIGH</b>	2	1
<b>LOW</b>	0,01	1

The actual experiments were carried out at 50°C, with different compositions of the HIGH (i.e. the geothermal brine) as given in Table 11. A similar approach as for the 3-compartment measurements was adopted: starting with pure NaCl solutions, testing the influence of Ca and Mg, both separately and combined, and finally testing a realistic brine, composited according to the information given in Table 3.

Table 11 Experimental conditions for the SGP-RE pilot testing

	LOW	HIGH	Temperature
<b>Experiment 1</b>	0,01M NaCl	0,05M MgCl <sub>2</sub> 1,95M NaCl	50°C
<b>Experiment 2</b>	0,01M NaCl	0,25M CaCl <sub>2</sub> 1,75M NaCl	50°C
<b>Experiment 3</b>	0,01M NaCl	0,05M MgCl <sub>2</sub> 0,25M CaCl <sub>2</sub> 1,70M NaCl	50°C
<b>Experiment 4</b>	0,01M NaCl	CaCl <sub>2</sub> , FeCl <sub>2</sub> , MgCl <sub>2</sub> , SrCl <sub>2</sub> , NaHCO <sub>3</sub> , Na <sub>2</sub> SO <sub>4</sub> , NaCl (*)	50°C
<b>Experiment 5</b>	Surface water	Geothermal brine Balmatt site in Mol (Belgium)	-

(\*) according to concentrations given in Table 3



## 4.2 Results and discussion

At the time of writing this deliverable the pilot experiments were still on-going. Results of the pilot test will be added in an updated version of this deliverable by the December 2018, when Task 3.3 ends.

## 5 Conclusions

A specific lab-scale setup to test a single cell pair SGP-RE system was designed and built for investigating the applicability of the process. Four steps were taken to elucidate the most important factors influencing the performance: examination of the performance of three commercially available membrane pairs (1), effect of increased temperature (2); effect of multivalent ions (3), combined effect of multivalent ions and increased temperature (4).

Testing three combinations of commercially available ion exchange membranes in the lab setup it revealed that FUJI membranes were the most performant at high salt concentration, but their performance dropped significantly when the brine concentration lowered. The other two pairs were more suitable at moderate to low concentrations and also less prone to a decrease in concentration of the brine.

The experiments at increased temperature showed a very clear benefit of using geothermal brines at 60°C or even higher. The power density of the FKE/FAS membranes at high temperatures increased 10 times compared to the tests at room temperature, even though the cell potential was less than expected due to a deteriorating permselectivity at high temperatures.

The final lab experiments consisted of determining the effect of multivalent ions on the performance. Calcium and Magnesium were chosen as the most common multivalent cations observed in real brines. The effect was studied on the FUJI and FKE/FAS membrane pairs. It was found that the presence of Ca and Mg had little or no effect on the cell potential (given equal molarities). As a single salt, neither Ca nor Mg had a big influence on the performance of the single cell. In a combined set of experiments however it was found that the performance reduced significantly when both cations ( $\text{Ca}^{2+}$ ,  $\text{Mg}^{2+}$ ) were present. In those cases the performance was reduced approximately 50%, compared to the case without multivalent ions. This performance loss was consistent throughout the entire temperature range that was studied (25-60°C).

## 6 References

- 1EIA, *International energy outlook 2011*. U.S. Department of Energy: Washington D.C., 2011; 301 p.
- Wick, G. L., *Power from salinity gradients*. *Energy* 1978, 3, (1), 95-100.
- 2Sanjuan, B., Millot, R., Dezayes, C., & Brach, M. (2010). Main characteristics of the deep geothermal brine (5km) at Soultz-sous-Forêts (France) determined using geochemical and tracer test data. *Comptes Rendus Geoscience*, 342(7-8), 546–559.
- 3R.E. Pattle, *Production of electric power by mixing fresh and salt water in the hydroelectric pile*, *Nature* 174 (1954) 660.
- 4 J.N. Weinstein, F.B. Leitz, *Electric power from differences in salinity: The dialytic battery*, *Science* 191 (1976) 557–559.
- 5 G.R. Wick, J.D. Isaacs, *Salt Domes: Is there more energy available from their salt than from their oil?* *Science* 199 (1978) 1436–1437.
- 6 R.E. Lacey, *Energy by reverse electrodialysis*, *Ocean Eng.* 7 (1980) 1–47.
- 7 S. Loeb, *Large-scale power production by pressure-retarded osmosis, using river water and sea water passing through spiral modules*, *Desalination* 143 (2002) 115–122.
- 8 E. Brauns, *Combination of a desalination plant and a salinity gradient power reverse electrodialysis plant and use thereof*, PCT/BE2006/000078, 2006.
- 9 E. Brauns, *Towards a worldwide sustainable and simultaneous large scale production of renewable energy and potable water through salinity gradient power by combining reversal electrodialysis and solar power ?*, *Desalination* 219 (2008) 312-323.
- 10 E. Brauns, *An alternative hybrid concept combining seawater desalination, solar energy and reverse electrodialysis for a sustainable production of sweet water and electrical energy*, *Desalination and Water Treatment* 13 (2010) 53-62.
- 11 J.W. Post, J. Veerman, H.V.M. Hamelers, G.J.W. Euverink, S.J. Metz, K. Nymeijer, C.J.N. Buisman, *Salinity-gradient power: Evaluation of pressure-retarded osmosis and reverse electrodialysis*, *J. Membr. Sci.* 288 (2007) 218–230.
- 12 J.W. Post, *Blue Energy, Electricity Production from Salinity Gradients by Reverse Electrodialysis*, PhD thesis, University of Wageningen, The Netherlands, November 3, 2009.
- 13 J.W. Post, H.V.M. Hamelers, C.J.N. Buisman, *Energy recovery from controlled mixing salt and fresh water with a reverse electrodialysis system*, *Environ. Sci. Technol.* 42 (2008) 5785–5790.
- 14 J.W. Post, H.V.M. Hamelers, C.J.N. Buisman, *Influence of multivalent ions on power production from mixing salt and fresh water with a reverse electrodialysis system*, *J. Membr. Sci.* 330 (2009) 65–72.
- 15 E. Brauns, *Salinity gradient power by reverse electrodialysis: effect of model parameters on electrical power output*, *Desalination* 237 (2009) 378–391.
- 16 E. Brauns, *Finite elements-based 2D theoretical analysis of the effect of IEX membrane thickness and salt solution residence time on the ion transport within a salinity gradient power reverse electrodialysis half cell pair*, *Desalination and Water Treatment*, Doi: 10.1080/19443994.2013.807905

17 H. Strathmann, *Ion-Exchange Membrane Separation Processes, Membrane Science and Technology Series, 9, Elsevier, 18 2004*

## 7 Glossary

AM	Anion exchange Membrane. Selective barrier allowing predominantly anions to pass through
CM	Cation exchange Membrane. Selective barrier allowing predominantly cations to pass through
SGP-RE	Salt Gradient Power through Reverse Electrodialysis
HIGH	refers to the brine solution and/or compartment in an SGP-RE stack or process
LOW	refers to the low salinity water sources and/or compartment in an SGP-RE stack or process
ELEC	refers to the electrode compartment or electrode rinsing solution of an SGP-RE stack or process. It contains generally an redox-couple and a supporting electrolyte
P&ID	Process and identification sheet
MeFiAS	Labview data acquisition and process control system developed by (VITO)
OCV	Open circuit voltage (V). This is the voltage of the stack under zero-load conditions when no current is flowing
R_stack	stack resistance ( $\Omega$ )
I_shortcut	Short cut current (A)
Pd	Power density expressed as electrical power output per $\text{m}^2$ of cell pair
Pd net	Net power density: power density minus hydraulic losses
Pd corr	Corrected power density: power density of the stack minus the power losses at the electrode